

BEAM BREAKUP (BBU) INSTABILITY EXPERIMENTS ON THE EXPERIMENTAL TEST ACCELERATOR (ETA)
AND PREDICTIONS FOR THE ADVANCED TEST ACCELERATOR (ATA)*

G. J. Caporaso, A. G. Cole and K. W. Struve
Lawrence Livermore National Laboratory
P. O. Box 808, L-321
Livermore, California 94550

In linear accelerators the maximum achievable beam current is often limited by the Beam Breakup (BBU) instability.¹ This instability arises from the interaction of a transversely displaced beam with the dipole modes of the accelerating cavities. The modes of interest, the TM_{1n0} modes, have non-zero transverse magnetic fields at the center of the cavity. This oscillating field imparts a time varying transverse impulse to the beam as it passes through the accelerating gap. Of the various modes possible only the TM_{130} mode has been observed on the Experimental Test Accelerator (ETA) and it is expected to surface on the Advanced Test Accelerator (ATA).²

The amplitude of the instability depends sensitively on two cavity parameters; Q and Z_{\perp}/Q . Q is the well-known quality factor which characterizes the damping rate of an oscillator. Z_{\perp}/Q is a measure of how well the beam couples to the cavity fields of the mode and in turn, how the fields act back on the beam. Lowering the values of both these parameters reduces BBU growth.

Efforts in reducing the severity of this mode have concentrated on reducing the Q of the accelerator cavities.³ By placing ferrite on the drive blades and back wall of the cavities, the Q 's were greatly reduced. It was found that the Q 's could be further reduced by placing a reflector in the corner of the accelerator cavity. A summary of the cavity Q 's and transverse impedances for the ETA and ATA cavities determined from bench tests is given in Table I. The transverse impedances given are the values measured on the ETA cavity and corrected for transit time effects. The transverse impedance of the ATA cavity was not measured. It is, however, not expected to differ from that of the ETA due to its similar design. A summary of the efforts to reduce the amplitude of the BBU oscillations is shown in Fig. 1.

TABLE I

Summary of Accelerator Cavity Q 's and Transverse Impedances

Mode	Frequency		ETA Q 's		ATA Q 's	
	(MHz)	Z_{\perp}/Q (ohms)	Undamped	Damped	Undamped	Damped
TM_{110}	345	8.2	40	*	-	*
TM_{120}	605	8.1	50	*	-	*
TM_{130}	830+	8.0	41	7	34	4

* Resonances looked for but not found

- Not studied

+ Resonant frequency reduced to 790 MHz in the damped cavity

Because of the difficulty in measuring the Q and transverse impedance of a very low Q resonance, the data in the table are uncertain to about $\pm 20\%$. For this reason tickler experiments were undertaken on the ETA to verify these values. In the following we describe the experiment and explain how these values were independently measured. Predictions for the ATA based on these results are then given.

Description of the Experiment

The physical layout of the ETA accelerator section is shown in Fig. 2. Shown are the eight accelerator cavities, various solenoidal focusing magnets, wall current monitors (also called "beam bugs"), the location of the rf B_0 pickup loops and the tickler cavity. The tickler is a high Q , offset rectangular

cavity which is inserted in the beamline upstream of the accelerator, (Fig. 3). The beam excites the TM_{110} mode of the tickler which produces a small rf transverse impulse on the beam at the mode frequency. The resulting amplitude of this modulation is measured by 4 rf loops located approximately one-half a cyclotron wavelength downstream. An additional set of 4 rf loops is located at the end of the accelerator. The ratio of output amplitude to input amplitude or gain was obtained in this manner. The tickler cavity contained a plunger which permitted tuning of its mode frequency so that gain could be determined as a function of frequency for frequencies near 800 MHz. The rf probes are single turn loops placed at the drift tube wall and oriented to intercept the beam generated B_0 field. The signal produced by the probe is a sum of contributions from the dI/dt of the beam and the dr/dt of the beam position. With a sinusoidal variation in the beam position $r_b = r + \Delta r \sin \omega t$,

$$V_{\text{probe}} = k \frac{d}{dt} \left(\frac{I}{r_b} \right) \approx \frac{k}{r} \left(\dot{I} - I \frac{\Delta r}{r} \cos \omega t \right) = V_I + V_{\text{rf}} \quad (1)$$

where $k = \mu_0 A \delta / 2\pi$, and δ is an empirically determined calibration factor of order 1/2. A is the loop cross sectional area. Both the dI/dt and dr_b/dt effects are easily seen in a typical signal. The large spikes near the beginning and end of the signal come from the rising and falling edges of the beam current. The oscillations in between, where dI/dt is small, come from the transverse motion of the beam centroid.

The beam bugs measure the electron beam current and centroid position versus time on time scales longer than that of the BBU.⁴ The beam bug is a resistive section of the beam tube wall across which the voltage drop from the return currents in the wall are measured.

For direct comparison with theory it is also necessary to know the beam energy and B_z tune throughout

the accelerator. The beam energy is determined from a sum of signals from each accelerating gap. The B_z field strength is determined by calculating the on-axis field of each coil and summing the contributions from all the coils. The field for each coil is determined from its shape and its measured DC current.

B_0 probe signals from all locations were simultaneously measured using 1 GHz bandwidth oscilloscopes (Tektronix 7104 with 7A29 and 7B10 plug-ins). This data along with simultaneous beam bug data provided a complete characterization of each shot. In this manner pulse-to-pulse variations in beam profile and current could be accounted for.

Data Analysis

The experimental data is compared against the results of a computer code which employs the single mode theory of Neil, Hall and Cooper¹ to calculate the growth of the instability. Each accelerating cavity is characterized by three parameters; the angular frequency of the dominant mode ω , its quality factor Q and its transverse shunt impedance Z_{\perp}/Q . The tickler experiment is basically an attempt to obtain a dynamic measurement of Z_{\perp}/Q and Q while the cavities are being operated in the ETA accelerator.

The code utilizes solenoidal transport which is able to incorporate the accelerator "tune" or actual axial variation of the magnetic field throughout the accelerator. In the calculation the accelerator is

divided into small (~ 4 cm) cells characterized by a constant magnetic field. The actual transport from cell to cell is represented by a 4×4 matrix which approximately treats the effects of fringing fields. The code models the variation of beam energy through the pulse by imposing a parabolic variation of γ such that at the beginning and end of the pulse the energy is down to 80% of its value at the middle of the pulse. The results obtained are not very different from the case of constant energy throughout the pulse. The energy of the beam as it exits the injector is an input parameter to the code as is the energy increase to the beam imparted by each cavity. The measured temporal profile of the beam current is input from digitized and smoothed beam-bug measurements. The results were not sensitive to the detailed shape of the current pulse, only to its amplitude.

The beam is assumed to be on center when it exits the injector. Because the tickler cavity is grossly asymmetric the effective displacement of the beam from the cavity center is 7.3 cm. The actual beam centroid is within 1 cm of the pipe axis at that axial location. The precise level of BBU impressed on the beam by the tickler in the code is not important since it is the ratio of the downstream BBU amplitude to the upstream BBU amplitude that is compared to experiment. In order to facilitate this comparison the code calculates the voltage waveforms that the rf loops at various positions down the accelerator should produce. Peak amplitudes are read off from each of the two sets of four rf loops. The 4 peak readings at each axial location are averaged and the gain computed. This figure is then directly compared with averages of several shots at each frequency. Fig. 4 shows the experimentally determined gain vs. frequency. Each data point is the average of from two to five shots.

Since the beam current actually decreased from approximately 9.7 kA to 8.5 kA through the accelerator the code runs were done with two different current values at each frequency. The average current at the beginning of the accelerator for that frequency was used to bracket the gain from above and the average current at the end of the accelerator was used to bracket the gain from below. The best fit was obtained with $Z_L/Q = 6$ ohms and $Q = 7$. The input and output current curves for this case are shown superimposed on the data of Fig. 4. The corresponding code points for $Z_L/Q = 8$ ohms and $Q = 7$ were roughly a factor of 2 higher than those shown. That is, the experiment was fairly sensitive to Z_L/Q . The results were not as sensitive to variations of Q at a fixed Z_L/Q . The final results for all the studies indicate that for ETA, $Z_L/Q = (6 \sim 7) \pm 1$ ohms, $Q = 7 \pm 1$.

Projections for ATA

The level to which the beam breakup amplitude grows depends crucially on several factors. These are beam current I , Z_L/Q , Q , mode frequency ω , number of cavities N , solenoidal magnetic field strength B and initial rf noise amplitude at the mode frequency ξ_0 .

An asymptotic formula valid at the end of ATA explicitly displays the dependences on these parameters.

$$\xi \propto \xi_0 \exp \left\{ \frac{K N I_{kA} Q (Z_L/Q) \omega}{B_{KG}} \right\}, \quad (2)$$

where $K = 1.16 \times 10^{-13}$ KGauss - sec/(kAmp-ohm).

The preliminary rf noise measurements on the ATA injector indicate that $\xi_0 \approx 1.8 \times 10^{-4}$ cm, comparable to the lowest ETA value observed. Taking Z_L/Q to be $(6 \sim 7) \pm 1$ ohms and Q to be 4 ± 1 for ATA the code projections are shown in Fig. 5. The calculation assumes a moderate field strength tune and the noise level quoted above.

There are many options for minimizing the growth of BBU in ATA. One of them involves raising the

injector voltage and accelerating voltages on the first 20 gaps. This would permit increasing the solenoidal magnetic field at the beginning of the accelerator without encountering difficulties with virtual cathode formation. Preliminary results indicate that this could reduce the values of Fig. 5 by up to a factor of 20.

In summary, the tickler experiment on ETA has permitted an improved determination of Z_L/Q and Q for the ETA cavities. The implications for ATA BBU growth have been discussed.

References

1. V. K. Neil, L. S. Hall, R. K. Cooper, Part. Accel. **9**, 213 (1979).
2. R. J. Briggs, et al., IEEE Trans. Nucl. Sci. **NS-28**, p. 3360, (1981).
3. G. J. Caporaso, K. W. Struve, Experimental Studies of the Beam Breakup Mode on ETA: Comparison with Theory, UCID-19402.
4. T. J. Fessenden, B. W. Stallard, G. G. Berg, Rev. Sci. Instrum. **43**, 1789 (1972).

*Performed jointly under the auspices of the U. S. DOE by LLNL under W-7405-ENG-48 and for the DOD under DARPA, ARPA Order #4395, monitored by NSWC.

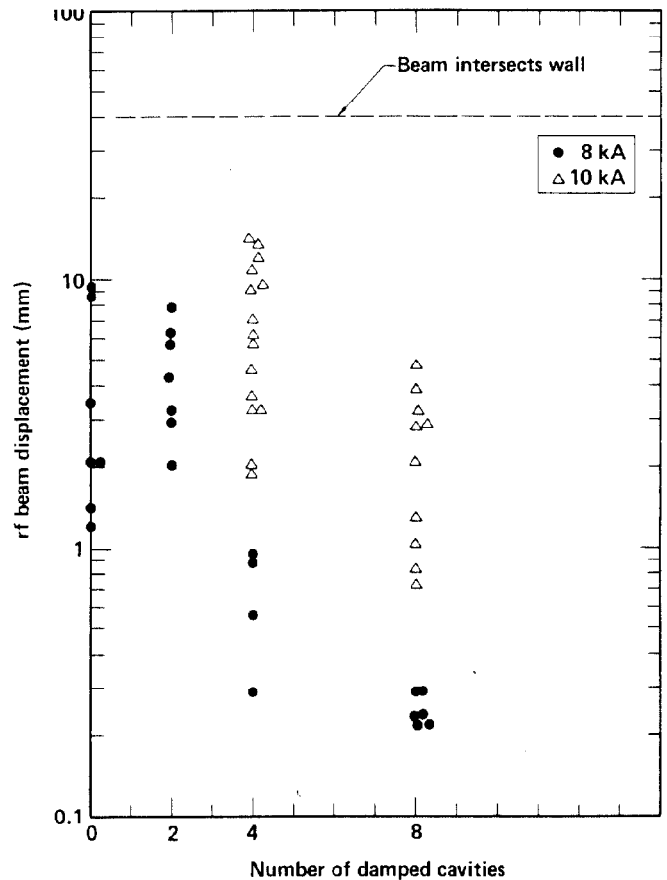


Fig. 1 Amplitude of the BBU oscillations of the ETA beam as a function of the number of damped accelerator cavities at both 8 and 10 kA. Each point represents 1 shot. The spread in amplitudes is due to pulse-to-pulse variations in beam conditions.

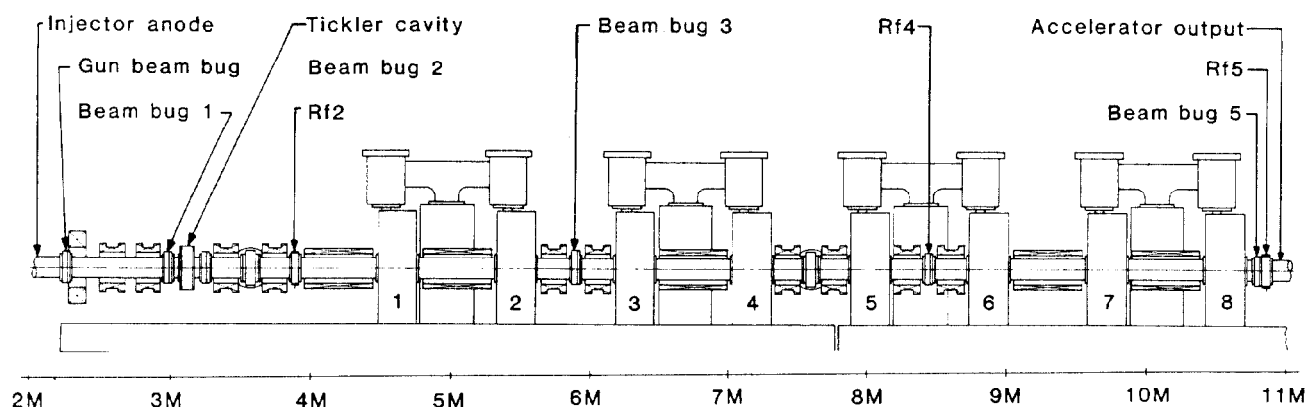


Fig. 2 Schematic of the ETA showing the location of the tickler cavity, upstream and downstream rf loop stations labeled RF 2 and RF 4 respectively and beam bugs.

CUTAWAY VIEW OF TICKLER CAVITY

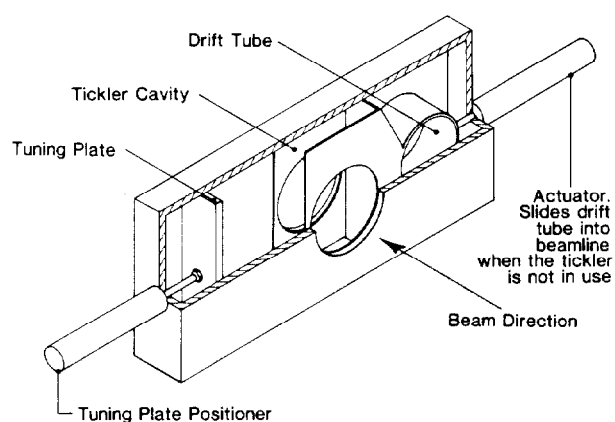


Fig. 3 Diagram of the tickler cavity showing the tuning plate and positioner. When not in use the tickler cavity can be replaced by a section of drift tube pushed into place by an actuator.

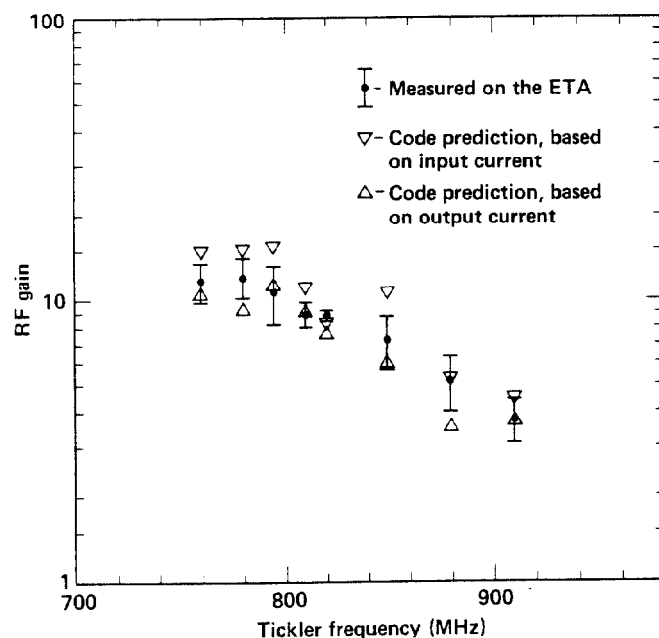


Fig. 4 Experimentally determined rf gain and code results vs. tickler frequency. Both cases have $Z_L/Q = 6$, $Q = 7$ which gave the best agreement with the data.

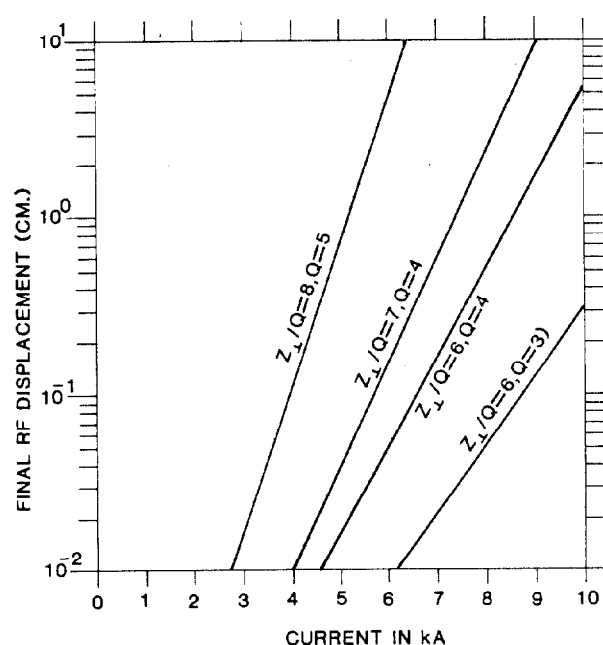


Fig. 5 Final rf displacement at the end of ATA vs. beam current for various values of cavity mode parameters. The shaded region represents the best estimate of ATA BBU growth based on Z_L/Q as determined from the tickler experiments and preliminary injector noise measurements on ATA. A nominal tune is assumed for the calculation.